nature neuroscience

Astrocytes control synaptic strength by two distinct v-SNARE-dependent release pathways

Yvonne Schwarz[1], Na Zhao[2], Frank Kirchhoff[2] & Dieter Bruns[1]

Communication between glia cells and neurons is crucial for brain functions, but the molecular mechanisms and functional consequences of gliotransmission remain enigmatic. Here we report that astrocytes express synaptobrevin II and cellubrevin as functionally non-overlapping vesicular SNARE proteins on glutamatergic vesicles and neuropeptide Y-containing large dense-core vesicles, respectively. Using individual null-mutants for *Vamp2* (synaptobrevin II) and *Vamp3* (cellubrevin), as well as the corresponding compound null-mutant for genes encoding both v-SNARE proteins, we delineate previously unrecognized individual v-SNARE dependencies of astrocytic release processes and their functional impact on neuronal signaling. Specifically, we show that astroglial cellubrevin-dependent neuropeptide Y secretion diminishes synaptic signaling, while synaptobrevin II–dependent glutamate release from astrocytes enhances synaptic signaling. Our experiments thereby uncover the molecular mechanisms of two distinct v-SNARE-dependent astrocytic release pathways that oppositely control synaptic strength at presynaptic sites, elucidating new avenues of communication between astrocytes and neurons.

Brain communication via vesicular exocytosis has long been considered to be specific to neuronal synapses. Accumulating evidence, however, suggests that astrocytes, beside their supportive functions in the brain, actively modulate synaptic transmission[1–7]. A single astrocyte can ensheath thousands of synapses[8], an arrangement that demands mutual interactions between neurons and astrocytes. The concept of the 'tripartite synapse' comprises presynaptic and postsynaptic elements together with an astroglial perisynaptic sheath, which receives input from and feeds backward on synaptic signaling[9]. Astrocytes detect neurotransmitters released during neuronal activity and, in turn, may modulate synaptic transmission by releasing neuroactive substances termed gliotransmitters[9–11]. Gliotransmitters such as glutamate, ATP, neuropeptide Y (NPY), D-serine or TNF-α[1,4,7,9,12–14] have the potential to regulate synaptic transmission and plasticity by either neuronal excitation or inhibition[1–6]. Yet the precise mode of gliotransmission and its impact on fast neuronal signaling has remained poorly understood. Indeed, even fundamental questions as to whether and how astrocytes release transmitters (for example, vesicular versus nonvesicular release) have remained controversial[10,11,15]. Previous studies have shown that astrocytes contain various exocytosis-competent intracellular organelles, such as glutamatergic small synaptic-like microvesicles (SLMVs), larger peptidergic vesicles and secretory lysosomes[11]. Yet no consensus has been reached on the expression and impact of major vesicular SNARE proteins like synaptobrevin II (VAMP2; sybII) or its homolog cellubrevin (VAMP3; ceb)[16–20]. While functional analyses with tetanus neurotoxin (TeNT) or the dominant-negative mouse model (dnSNARE) provide evidence for exocytotic release of gliotransmitters, they failed to discriminate between sybII- or ceb-mediated exocytosis, because both v-SNARE proteins are similarly cleaved by the endoprotease TeNT or hindered by truncated v-SNARE fragments in mediating fusion[1,2,5].

Here we show that astrocytes express sybII and ceb on distinct vesicle populations, where they act in a functionally non-overlapping fashion, mediating glutamate and NPY release, respectively, through distinct secretion pathways. Taking advantage of single and double v-SNARE knockout mice, in combination with electrophysiological and imaging analyses of synaptic transmission, we show that sybII- and ceb-mediated release of gliotransmitters oppositely regulates synaptic strength by influencing fundamental presynaptic parameters, such as the number of readily releasable vesicles and the release probability. Taken together, our results elucidate previously unrecognized molecular mechanisms of two independent astrocytic secretion pathways that are able to fine-tune neuronal signaling and may represent an integral part of bidirectional neuron–astrocyte communication.

RESULTS

SybII and ceb mediate distinct secretion pathways in astrocytes

In a first set of experiments, we investigated whether the major v-SNARE proteins sybII and ceb are expressed in cultured hippocampal astrocytes. Co-immunolabeling revealed that both v-SNAREs are expressed in astrocytes but are sorted to distinct subcellular organelles (**Supplementary Fig. 1a**). While sybII was preferentially found at the cell's periphery, ceb was scattered throughout the cytoplasm. No staining could be observed in null-mutants for the corresponding antigens, confirming the specificity of the affinity-purified antibodies (**Supplementary Fig. 2**). Line-scan analyses, cytofluorograms and a low Mander's coefficient confirmed the distinct localization of both v-SNAREs in astrocytes (**Supplementary Fig. 1d–f**). Notably, ceb strongly co-localized with the endogenous large dense core vesicle (LDCV) marker protein NPY[13], whereas sybII was sorted to vGlut$^+$ glutamatergic vesicles (**Supplementary Fig. 1b–d**). Taken together, astrocytes express the two v-SNARE isoforms, sybII and ceb,

[1]Molecular Neurophysiology, Center for Integrative Physiology and Molecular Medicine, Saarland University, Homburg, Germany. [2]Molecular Physiology, Center for Integrative Physiology and Molecular Medicine, Saarland University, Homburg, Germany. Correspondence should be addressed to D.B. (dieter.bruns@uks.eu).

Received 30 January; accepted 24 August; published online 25 September 2017; doi:10.1038/nn.4647

on distinct vesicle populations that contain either classical or peptidergic cargo molecules, respectively.

To investigate the v-SNARE dependence of vesicular exocytosis, we transfected astrocytes with fluorescently tagged NPY (using monomeric teal fluorescent protein). These tagged NPY puncta were visible throughout the cell (**Fig. 1a**), agreeing well with endogenous NPY staining (**Supplementary Fig. 1b**). Superfusion of astrocytes with glutamate strongly decreased the number of NPY puncta in wild-type (WT) cells, providing evidence for exocytotic release (**Fig. 1a–c**). No NPY release was observed in the absence of glutamate stimulation (**Fig. 1b**) or during simultaneous incubation with a metabotropic glutamate-receptor antagonist, MPEP (2-methyl-6-(phenylethynyl)-pyridine, 10 µM; **Fig. 1d**). For sybII-knockout (sybII-ko) astrocytes, NPY secretion was indistinguishable from WT cells, whereas it was completely abolished in ceb-knockout (ceb-ko) astrocytes. These functional results agree well with the high degree of co-localization between NPY and ceb (**Supplementary Fig. 1b**). Accordingly, in sybII and ceb double-knockout (dko) cells, NPY release was similarly abrogated (**Fig. 1d,e**). In accordance with the phenotypes of the single v-SNARE deficiencies, expression of ceb but not sybII in dko astrocytes led to a gain-of-function phenotype by restoring NPY secretion to the level of WT cells (**Fig. 1d,e**). Co-immunolabeling

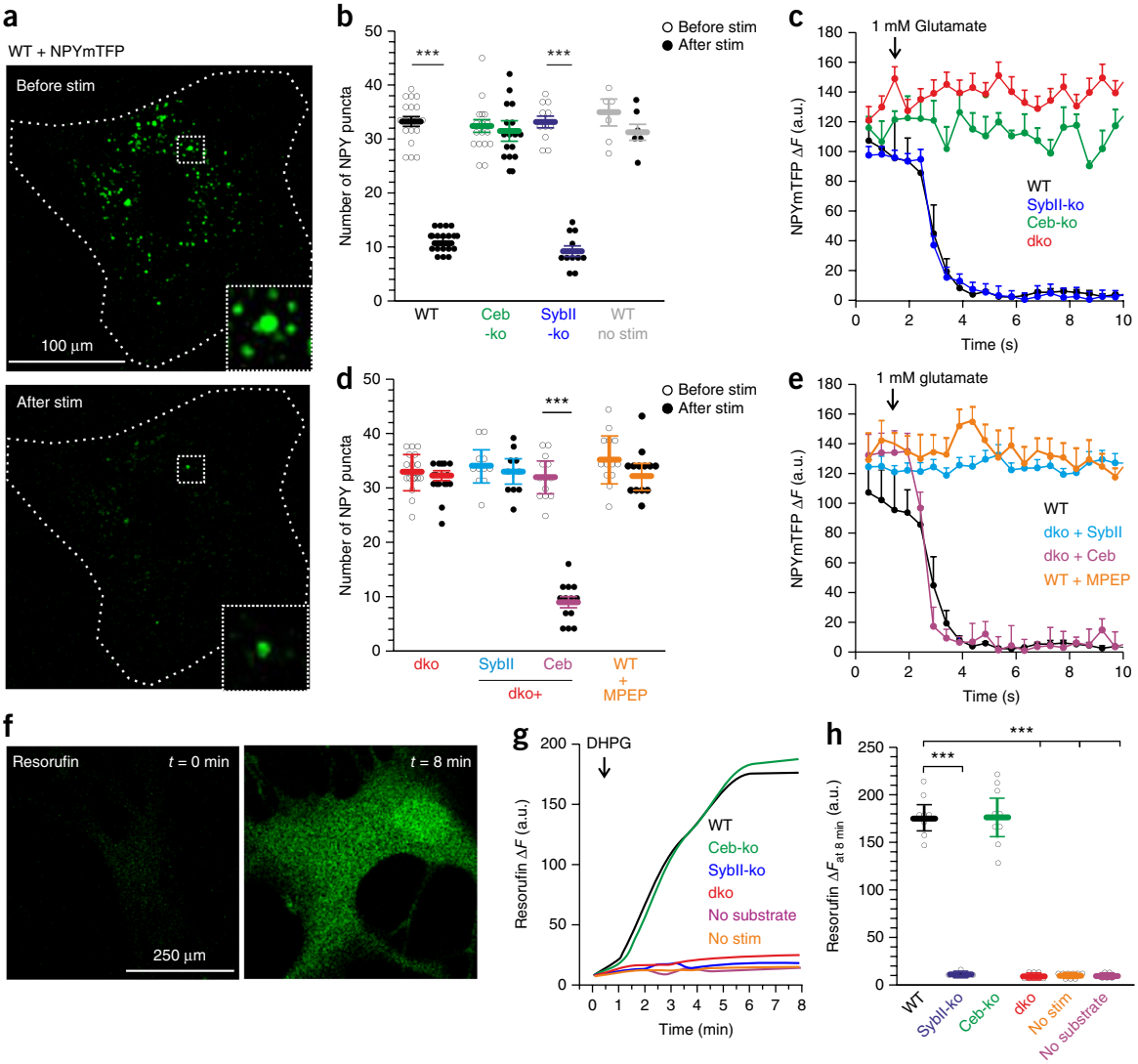

Figure 1 SybII and ceb govern distinct release pathways in astrocytes. (**a**) Example confocal images of a WT astrocyte expressing NPY tagged with monomeric teal fluorescent protein (NPYmTFP), illustrating the stimulation-dependent (1 mM glutamate) disappearance of NPYmTFP puncta. Dotted line represents the outline of the cell. Inset shows areas outlined in white dashed boxes. (**b**) Quantification of the number of NPY puncta before and after stimulation in a 50 × 50-µm region of interest (ROI). NPY secretion is abolished in ceb-ko and dko astrocytes (WT, $n = 19$; $P = 0.00078$; sybII-ko, $n = 11$; $P = 0.00034$; ceb-ko, $n = 13$; $P = 0.121$; WT, no stim = 6; $P = 0.65$, Student's t test). (**c**,**e**) Time course of NPYmTFP secretion from cells stimulated with 1 mM glutamate. (**d**) Expression of ceb but not sybII restores NPY secretion in dko astrocytes (Data was collected from three preparations; before stim vs. after stim: dko $n = 7$; $P = 0.00012$; dko + sybII, $n = 12$; $P = 0.43$; dko + ceb, $n = 13$; $P = 0.00054$; WT + MPEP, $n = 8$; $P = 0.124$, Students t test). (**f**) Exemplary images of resorufin fluorescence before and after stimulation with 10 µM DHPG (left, before stimulation; right, after stimulation). (**g**) Time-courses of the resorufin signal in astrocytes for the indicated groups. Note that glutamate secretion is abolished in sybII-ko but unchanged in ceb-ko astrocytes. Cells were stimulated using 10 µM DHPG (arrow). (**h**) Quantification of the resorufin signal 8 min after onset of stimulation (data was collected from three preparations; WT, $n = 8$; sybII-ko, $n = 7$, $P < 0.001$; ceb-ko, $n = 9$, $P = 0.35$; dko, $n = 8$, $P < 0.001$; no stim, $n = 9$, $P < 0.001$; no substrate, $n = 5$, $P < 0.001$, $^{***}P < 0.001$, one-way ANOVA vs. WT). All data are represented as mean ± s.e.m.

against ceb and NPY confirmed that only ceb-mRFP was specifically sorted to peptidergic vesicles (**Supplementary Fig. 3a**,**b**). Notably, the ability of the different v-SNARE-deficient astrocytes to generate similar intracellular Ca^{2+} signals in response to glutamate stimulation (**Supplementary Fig. 3c**–**e**) suggests that v-SNARE deficiency does not interfere with metabotropic glutamate-receptor trafficking. Thus, NPY secretion from astrocytes specifically depends on a ceb-mediated exocytotic release process.

To identify the v-SNARE protein responsible for astrocytic glutamate secretion, we adapted an assay wherein released glutamate serves as a substrate for a fluorometric enzyme, resulting in production of fluorescent resorufin molecules[21] (**Fig. 1f**,**g**). Stimulating WT astrocytes with the metabotropic receptor agonist dihydroxyphenylglycine (DHPG, 20 µM[22]) caused a strong increase in extracellular resorufin fluorescence (**Fig. 1g**,**h**). A similar result was obtained for ceb-ko cells, but no signal increase could be detected in either sybII-ko or dko astrocytes. Control experiments, without stimulation or in the absence of glutamate-converting enzymes, showed negligible fluorescence, confirming that resorufin signals reflect glutamate release from astrocytes. Collectively, these results indicate that sybII specifically promotes astrocytic glutamate release.

To monitor glutamate secretion directly, we transfected WT and various v-SNARE-knockout astrocytes with the genetically encoded glutamate sensor iGluSnFr (intensity-based glutamate-sensing fluorescent reporter)[23]. Cells were stimulated with 20 µM DHPG and superfused at the end of the experiment with 1 mM glutamate to provide an estimate of iGluSnFr expression (**Supplementary Fig. 4a**–**f**). In WT cells, DHPG evoked discrete, transient fluorescence events (**Supplementary Fig. 4**), which were abolished in the presence of MPEP (50 µM). The frequency of glutamate flashes was unaltered for ceb-ko astrocytes but strongly reduced in sybII-ko and dko astrocytes. The pulsatile, quantal-like character of the events, their magnitude and time course were indicative of the vesicular origin of glutamate and compared well with experiments showing iGluSnFr signals reporting spontaneous vesicular glutamate release in the mouse retina[23]. Secretion in response to DHPG showed a rapid onset and persisted during stimulation. These results confirm that sybII mediates astrocytic glutamate secretion. Notably, possible alterations in the expression level of iGluSnFr cannot be responsible for the different responses of the v-SNARE-deficient cells, because fluorescence signals evoked with external glutamate application were unchanged for all groups (**Supplementary Fig. 4d**). Furthermore, iGluSnFr-transfected sybII-ko neurons (which are devoid of glutamate secretion[24]) showed no action potential (AP)-evoked fluorescence increase (in contrast to controls), confirming the validity of the iGluSnFr measurements (**Supplementary Fig. 4g**–**j**). Taken together, these experiments provide direct evidence that sybII and ceb mediate, in a functionally non-overlapping manner, the astrocytic release of NPY and glutamate, respectively.

v-SNARE-dependent release from astrocytes modulates synaptic efficacy

To investigate how loss of either pathway influences neuronal glutamatergic signaling, we used autaptic hippocampal neuron cultures grown on either WT or various v-SNARE-knockout astrocytes (**Fig. 2a**). Notably, genetic ablation of the gene encoding sybII in astrocytes significantly reduced both the frequency of miniature excitatory postsynaptic currents (mEPSCs) and the AP-evoked response (EPSC) in single, autaptic WT neurons, suggesting that impaired glutamate secretion from astrocytes diminishes synaptic efficacy (**Fig. 2b**–**e**). In stark contrast, loss of ceb strongly increased evoked-EPSC

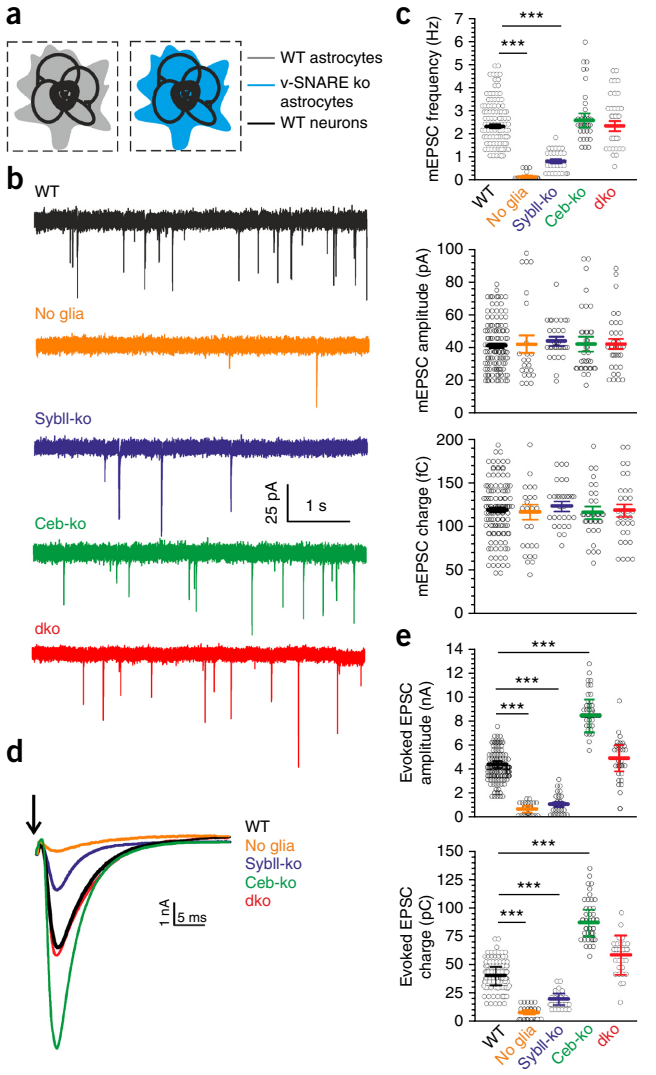

Figure 2 v-SNARE-mediated gliotransmitter release from astrocytes modulates synaptic efficacy. (**a**) Schematic drawing of the autaptic neuronal culture. Neurons were grown either in the absence of glia cells or on astrocytes derived from single or double v-SNARE-knockout mice. (**b**) Exemplary traces of spontaneous mEPSC recordings in neurons cultured without glia or on WT, sybII-ko, ceb-ko and dko astrocytes. (**c**) Analysis of the averaged mEPSC frequency, amplitude and charge for all groups. Note that only the absence of glia or the loss of sybII in astrocytes causes a strong decrease in the mEPSC frequency in neurons (mEPSC frequency: WT vs. no glia, $P = 0.00012$; WT vs. sybII-ko, $P = 0.0011$; WT vs. ceb-ko, $P = 0.32$; WT vs. dko, $P = 0.54$; mEPSC amplitude: WT vs. no glia, $P = 0.31$; WT vs. sybII-ko, $P = 0.36$; WT vs. ceb-ko, $P = 0.43$; WT vs. dko, $P = 0.13$; mEPSC charge: WT vs. no glia, $P = 0.54$; WT vs. sybII-ko, $P = 0.37$; WT vs. ceb-ko, $P = 0.46$; WT vs. dko, $P = 0.34$, one-way ANOVA). (**d**) Exemplary recordings of the AP evoked EPSCs (0.2 Hz) for the groups described in **b**. Arrow indicates the AP-evoked depolarization. Depolarization artifacts have been omitted for illustrative purposes. (**e**) EPSC amplitude (ampl.) and charge are significantly reduced in the absence of astrocytes or with sybII-ko astrocytes. The evoked response is strongly increased for astrocytic ceb-deficiency but remains unaffected by the loss of both v-SNARE proteins in astrocytes. (EPSC ampl.: no glia, $P = 0.000037$; sybII-ko, $P = 0.000032$; ceb-ko, $P = 0.000048$; dko, $P = 0.24$; EPSC charge: no glia, $P = 0.0008$; sybII-ko, $P = 0.00032$; ceb-ko, $P = 0.00029$; dko, $P = 0.073$, one-way ANOVA vs. WT). Data was collected from neurons cultured with WT ($n = 122$), no glia ($n = 24$), sybII-ko ($n = 32$), ceb-ko ($n = 38$) and dko ($n = 33$) astrocytes from three preparations. $^{***}P < 0.001$. All data are represented as mean ± s.e.m.

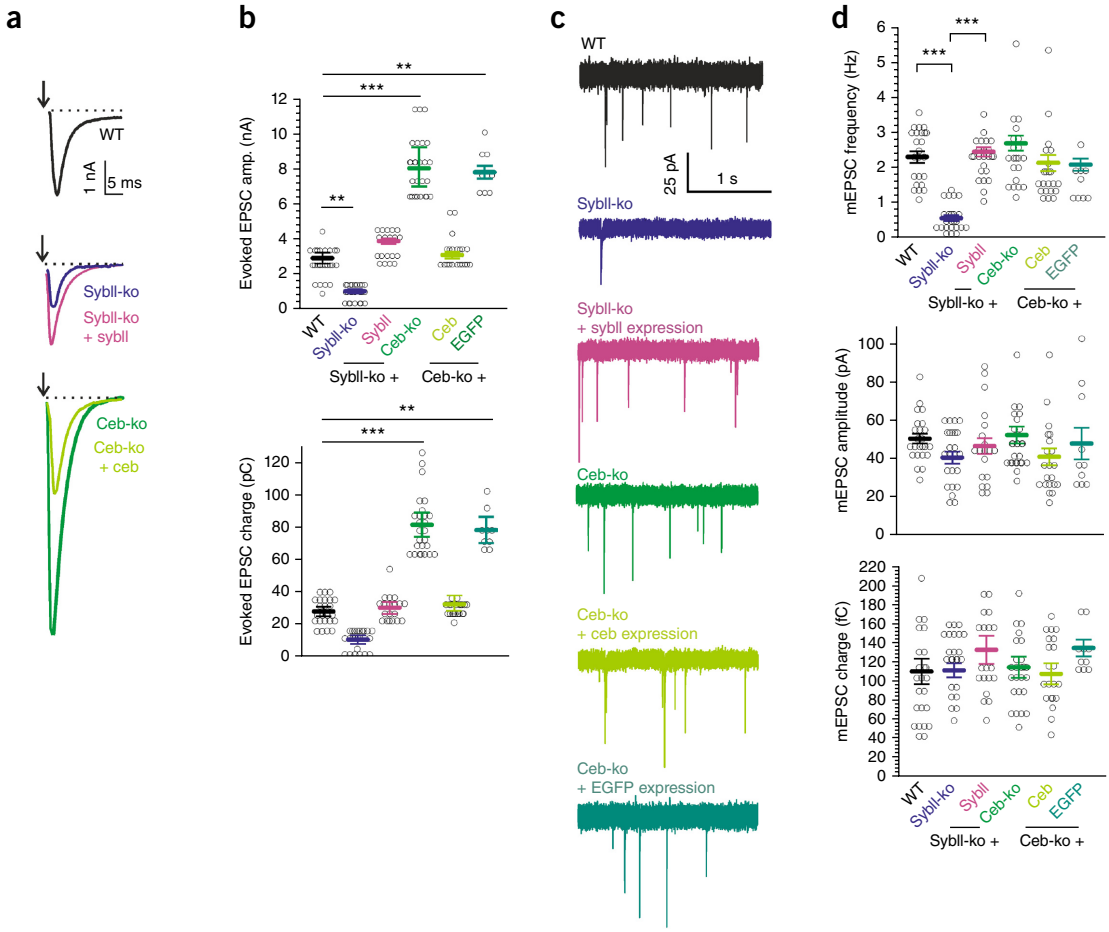

Figure 3 Expression of v-SNARE proteins in their respective knockout astrocytes completely restored the synaptic response to that measured from WT astrocytes. (**a**) Representative recordings of the AP-evoked response in neurons cultured on WT, ceb-ko, ceb-ko transfected with ceb, sybII-ko and sybII-ko transfected with sybII astrocytes. Arrows indicate AP-evoked depolarization. Depolarization artifacts have been omitted; dashed line indicates baseline. (**b**) EPSC amplitude and charge for the indicated groups. Expression of the v-SNARE protein in its respective knockout astrocyte completely restored the synaptic response to that measured from WT astrocytes. (EPSC ampl.: sybII-ko, $P = 0.0013$; sybII-ko + sybII, $P = 0.23$; ceb-ko, $P = 0.00046$; ceb-ko + ceb, $P = 0.13$; ceb-ko + EGFP, $P = 0.0012$; EPSC charge: sybII-ko, $P = 0.028$; sybII-ko + sybII, $P = 0.38$; ceb-ko, $P = 0.000052$; ceb-ko + ceb, $P = 0.43$; ceb-ko + EGFP, $P = 0.0017$, one-way ANOVA vs. WT). (**c**) Exemplary traces of spontaneous mEPSC recordings in autaptic hippocampal neurons for the groups described in **a**. (**d**) Analyses of mEPSC frequency (freq.), amplitude and charge shows that expression of sybII in sybII-ko astrocytes fully restores the mEPSC frequency to that recorded with WT astrocytes (data was collected from three preparations; WT, $n = 24$; ceb-ko, $n = 26$; ceb-ko + ceb, $n = 21$; ceb-ko + EGFP, $n = 9$; sybII-ko, $n = 24$; sybII-ko + sybII, $n = 19$; mEPSC freq.: sybII-ko, $P = 0.00004$; sybII-ko + sybII, $P = 0.28$; ceb-ko, $P = 0.32$; ceb-ko + ceb, $P = 0.43$; ceb-ko + EGFP, $P = 0.46$; mEPSC ampl.: sybII-ko, $P = 0.38$; sybII-ko + sybII, $P = 0.42$; ceb-ko, $P = 0.21$; ceb-ko + ceb, $P = 0.73$; ceb-ko + EGFP, $P = 0.21$; mEPSC charge: sybII-ko, $P = 0.18$; sybII-ko + sybII, $P = 0.28$; ceb-ko, $P = 0.19$; ceb-ko + ceb, $P = 0.32$; ceb-ko + EGFP, $P = 0.48$, one-way ANOVA vs. WT). $^{**}P < 0.01$, $^{***}P < 0.001$. All data are represented as mean ± s.e.m.

amplitudes, without changing mEPSC frequency. Still, loss of both sybII- and ceb-mediated secretion pathways left quantal signaling and evoked secretion unchanged when compared to controls (**Fig. 2**). These results indicate that sybII- and ceb-mediated gliotransmission antagonistically regulates rapid glutamatergic signaling. Furthermore, they suggest that the functional consequences of the distinct secretion pathways are noticeably well-balanced in the context of WT astrocytes. These observations are compatible with the finding that NPY strongly depresses evoked transmission but leaves quantal signaling unchanged[25]. Furthermore, they support observations that glutamate release from astrocytes can facilitate synaptic transmission acting either on presynaptic metabotropic[6,26,27] kainate[28] or NMDA receptors[2,22]. Evidently, the opposite effects of the different gliotransmitters demand independent astrocytic secretion pathways equipped with functionally non-overlapping v-SNARE proteins.

The general absence of glial cells, in contrast to the dko phenotype, strongly reduced the mEPSC frequency and the AP-evoked response (**Fig. 2**), an observation consistent with the profound influence of astrocytes on synapse development[29]. Conversely, we found that v-SNARE-dependent release pathways did not affect synaptogenesis, as discussed below. Thus, astrocytic v-SNARE-dependent control of neuronal signaling represents a mode of synaptic regulation that mechanistically differs from supporting functions by astrocytes in synapse development.

To test whether changes in synaptic efficacy are due to loss of glial v-SNARE proteins and are not a consequence of developmental alterations, we transfected astrocytes of v-SNARE null-mutants with the corresponding v-SNARE variant before co-culturing them with WT neurons. In agreement with our secretion analyses (**Fig. 1d**,**e**), ceb expression in ceb-ko astrocytes reduced evoked-EPSC amplitudes to

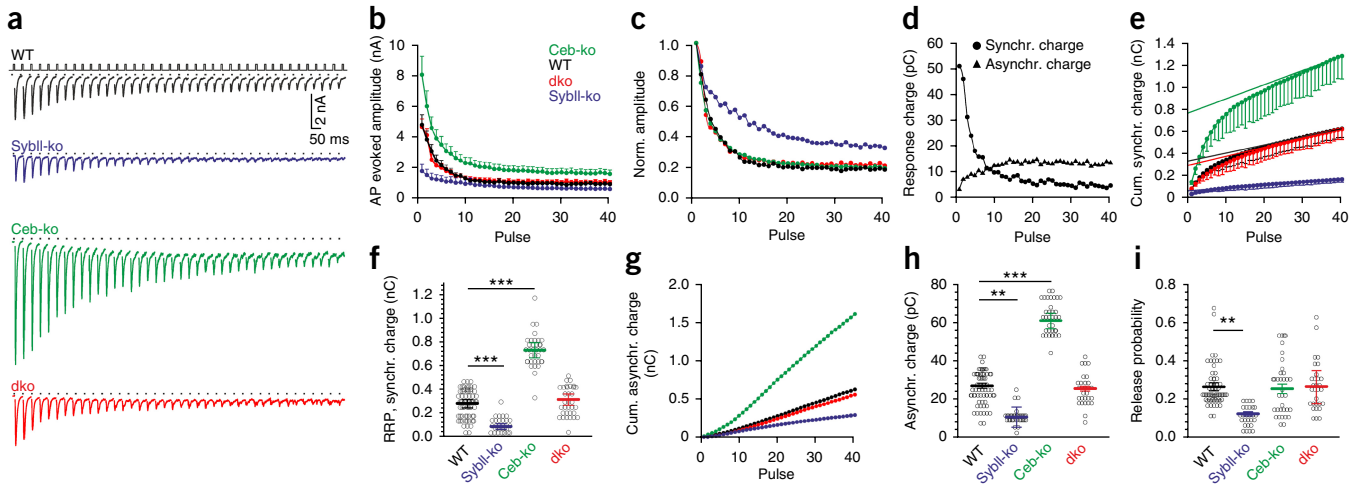

Figure 4 Gliotransmission modulates the readily releasable pool size and release probability in hippocampal neurons. (**a**) Representative EPSCs triggered by high-frequency stimulation (HFS; 20 Hz, 40 AP per 2 s) of autaptic neurons cultured on WT, sybII-ko, ceb-ko and dko astrocytes. (**b**) Averaged EPSC amplitudes plotted over the stimulus number. (**c**) The time-course of synaptic depression was reduced in neurons grown on sybII-ko astrocytes (data were normalized to the initial peak EPSC amplitude). (**d**) Estimates of synchronous and asynchronous release plotted against the stimulus. (**e**) Mean cumulative synchronous release components during a 20-Hz train. Data points from the linear component were back extrapolated to pulse = 0 to estimate the initial RRP size. (**f**) The RRP recorded in neurons cultured on sybII-ko astrocytes was reduced, whereas it was increased with ceb-ko astrocytes (sybII-ko, $P < 0.001$; ceb-ko, $P < 0.001$; dko, $P = 0.46$, one-way ANOVA vs. WT). (**g**,**h**) Mean cumulative asynchronous release for the indicated groups. Neuronal asynchronous release is also affected by v-SNARE-dependent secretion processes from astrocytes. Asynchronous release was determined as the mean charge over the last five stimuli. (sybII-ko, $P < 0.001$; ceb-ko, $P < 0.001$; dko, $P = 0.32$, one-way ANOVA vs. WT). (**i**) The release probability (first $EPSC_{charge}/RRP_{charge}$) was specifically decreased in sybII-ko astrocytes (sybII-ko, $P = 0.021$; ceb-ko, $P = 0.18$; dko, $P = 0.13$, one-way ANOVA vs. WT). Data was collected from WT, $n = 62$; sybII-ko, $n = 28$; ceb-ko, $n = 35$; dko, $n = 29$ from three preparations. $^{**}P < 0.01$; $^{***}P < 0.001$. All data are represented as mean ± s.e.m.

levels found with WT astrocytes, without changing the properties of quantal signaling (**Fig. 3**). In contrast, transfection with enhanced GFP (EGFP) failed to reduce the evoked response, demonstrating that ceb expression, rather than off-target effects of lentiviral transfection, was responsible for the observed phenotype. SybII expression in sybII-ko astrocytes, instead, elevated the mEPSC frequency and rescued the AP-evoked response to that observed with WT cells (**Fig. 3**). Collectively, these results indicate that expression of either v-SNARE variant in astrocytes restored the corresponding secretion pathway and its functional impact on synaptic signaling.

Astrocytes regulate the readily releasable pool size and release probability of hippocampal neurons

To elucidate the mechanisms by which synaptic release is regulated by gliotransmission, we used high-frequency train stimulations (20 Hz for 2 s) and comparatively analyzed the readily releasable pool (RRP) size, release probability (P_r) and synaptic depression. In good agreement with the results obtained with basal stimulation (0.2 Hz; **Fig. 2d**,**e**), the first AP-evoked response of the train was substantially decreased for neurons growing on sybII-ko astrocytes, whereas it was strongly enhanced with ceb-ko and unchanged for dko cells (**Fig. 4a**,**b**). Evoked synaptic responses of neurons grown on WT, ceb-ko and dko astrocytes displayed depression over the first ten APs before reaching an apparent steady state for the remaining stimuli of the train (**Fig. 4a–c**). In contrast, neurons cultured with sybII-ko astrocytes displayed a slower time-course and reduced synaptic depression, indicative for changes in vesicular P_r (**Fig. 4c**). To determine the RRP size, the plot of the cumulative synchronous EPSC charge was approximated with a linear regression fitting the last five stimuli (**Fig. 4e**). Back-extrapolating the linear component of the steady-state phase renders an estimate of the initial RRP size[30] (**Fig. 4e**,**f**). For sybII-ko astrocytes, the RRP size was significantly reduced, whereas it was strongly increased or unchanged with ceb-ko and dko astrocytes, respectively (**Fig. 4e**,**f**). Similarly, the asynchronous release component, which increased during the stimulus train due to accumulation of presynaptic intracellular $[Ca^{2+}]$, was found to be diminished with sybII-ko and increased with ceb-ko astrocytes (**Fig. 4d**,**g**,**h**). In contrast, P_r (determined by the ratio of the first EPSC charge to the RRP charge) was significantly reduced with sybII-ko astrocytes but remained unchanged for all other groups (**Fig. 4i**). Consistently, the paired-pulse facilitation (PPF), which is inversely related to P_r, only increased for neurons grown on sybII-ko astrocytes (**Supplementary Fig. 5d**,**e**). Experiments with hypertonic sucrose to determine the RRP size[31] with Ca^{2+}-independent stimulation confirmed the different impacts of sybII- and ceb-mediated release from astrocytes on RRP size and P_r (**Supplementary Fig. 5a–c**). Taken together, these v-SNARE-dependent release pathways from astrocytes oppositely regulate fundamental parameters of synaptic efficacy.

NPY and ATP mimic the inhibition by ceb-mediated gliotransmission

To explore whether loss of astrocytic NPY secretion can mimic the phenotype of ceb-ko astrocytes, we analyzed the impact of astrocytes derived from $NPY^{-/-}$ mice[32] (**Fig. 5**). Loss of astrocytic NPY significantly increased evoked-EPSC amplitude and charge, as well as the RRP size, albeit to a lesser degree than that found for ceb-ko cells (**Fig. 5a**,**b**). In contrast, mEPSC properties remained unchanged (**Fig. 5c**,**d**). While these results agree with previous reports showing that NPY diminishes neuronal transmission[25,32], they also suggest that other inhibitory gliotransmitters are additionally released in a ceb-dependent manner. Astrocytic ATP has been implicated in heterosynaptic depression[5,7] and was found to be present in the same subcellular fractions as the LDCV marker-proteins secretogranin II and chromogranin, which were distinct from fractions containing

sybII[33]. In following this up, we cultured neurons grown on ceb-ko astrocytes in the presence of either 10 nM NPY or a mixture of 10 nM each NPY and ATP. While NPY-only treatment partially reduced synaptic signaling (**Fig. 6a–c**), co-application of both NPY and ATP diminished evoked-EPSC amplitudes and the RRP size to levels found in WT astrocytes (**Fig. 6d–f**). These results provide strong evidence that NPY and ATP secreted from astrocytes generate an ambient inhibitory tone that impairs synaptic transmission. Similarly to findings described above, properties of quantal signaling remained unaltered (**Supplementary Fig. 6**), suggesting unchanged postsynaptic signal generation. Furthermore, acute NPY + ATP application (60 s perfusion time) strongly attenuated evoked-EPSC amplitudes and RRP size when compared with the preceding control response of the same neuron (**Supplementary Fig. 7a–c**). Adenosine (converted from ATP by ectonucleotidase activity[5]) has been implicated in mediating synaptic inhibition by tonic activation of presynaptic adenosine A1 receptors[34]. Likewise, NPY predominantly exerts its action through presynaptic NPY Y2 receptors, leading to reduced Ca^{2+} influx[35]. To further explore these mechanisms, we treated autaptic cultures with a mixture of 150 nM adenosine A1-receptor antagonist DPCPX and 150 nM NPY Y2-receptor antagonist BIIE0246. Neurons cultured with WT astrocytes showed a strong increase in their evoked response and RRP size (**Fig. 6g–i**), unmasking the tonic synaptic suppression by astrocytic NPY and ATP and/or adenosine. In good agreement with this finding, neurons grown on ceb-ko astrocytes, which are devoid of NPY and ATP secretion, were unaffected by treatment with the antagonists (**Fig. 6g,i**). Similarly to the chronic application, acute antagonist treatment (500 nM each DPCPX and BIIE0246) strongly and reversibly increased evoked responses in neurons grown on WT astrocytes but not in those cultured with ceb-ko cells (**Supplementary Fig. 7d–f**). Thus, ambient NPY and ATP, released in a ceb-dependent manner from astrocytes, tonically suppress synaptic transmission.

In particular, tonically activated presynaptic kainate receptors (KAR) and NMDA receptors have been implicated in enhancing neurotransmitter release[28,36]. Since NMDA receptors were chronically blocked in our experiments (preventing long-term plasticity changes), we tested whether astrocytic glutamate activates presynaptic KAR. The KAR antagonist NS-102 (3 µM)[37] produced a strong, reversible depression of the evoked response in neurons grown on WT astrocytes. Conversely, evoked EPSCs of neurons cultured with sybII-ko cells were unaltered, as expected for antagonist treatment in the absence of astrocytic glutamate release. The latter result also renders unlikely the possibility that NS-102 caused an off-target inhibition of AMPA receptors (**Supplementary Fig. 7g–i**). Collectively, these results demonstrate that ambient astrocytic glutamate facilitates synaptic efficacy.

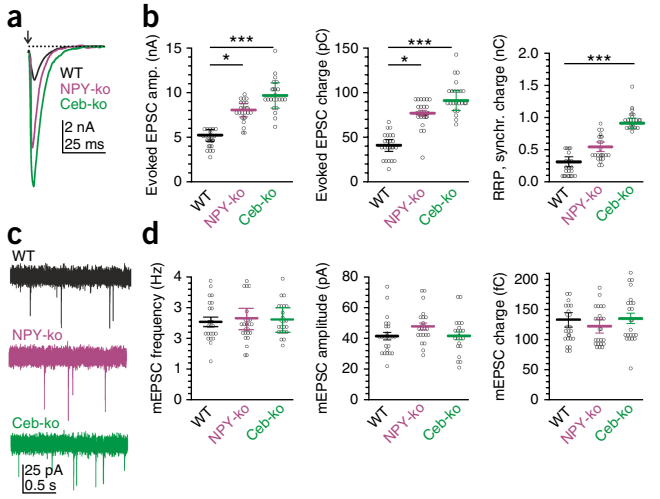

Figure 5 Loss of NPY secretion from astrocytes partially mimics the ceb-ko phenotype. (**a**) Representative recordings of AP-evoked EPSCs from neurons grown on WT, NPY-knockout (NYP-ko) and ceb-ko astrocytes. (**b**) Evoked neuronal amplitude, charge and readily releasable pool size are significantly increased in the absence of NPY but not as strongly as with ceb-deficiency (EPSC ampl.: NPY-ko, $P = 0.049$; ceb-ko, $P < 0.0001$; EPSC charge: NPY-ko, $P = 0.032$; ceb-ko, $P < 0.001$; RRP charge: NPY-ko, $P = 0.32$; ceb-ko, $P < 0.001$, one-way ANOVA vs. WT). (**c**) Exemplary traces of spontaneous mEPSC recordings from the groups described in **a**. (**d**) mEPSC frequency, amplitude and charge for the individual groups. Loss of neither astrocytic NPY nor ceb affects quantal signaling (mEPSC freq.: NPY-ko, $P = 0.32$; ceb-ko, $P = 0.23$; mEPSC ampl., WT vs.: NPY-ko, $P = 0.63$; ceb-ko, $P = 0.58$; mEPSC charge: NPY-ko, $P = 0.54$; ceb-ko, $P = 0.38$, one-way ANOVA vs. WT). Data were obtained from cultures with WT ($n = 24$), NPY-ko ($n = 24$), and ceb-ko ($n = 23$) astrocytes from three preparations. $^*P < 0.05$; $^{***}P < 0.001$. All data are represented as mean ± s.e.m.

v-SNARE-dependent astrocytic release regulates synaptic strength but not synaptogenesis

Astrocytes profoundly regulate synapse development and maintenance[29,38]. Thus, the neuronal phenotypes observed with different v-SNARE-deficient astrocytes may reflect changes in synapse number or alterations in synaptic efficacy (for example, the number of readily releasable vesicles per synapse). To delineate the underlying mechanism, autaptic neurons were transfected with the presynaptic marker protein synaptophysin-pHluorin. Here the vesicular membrane protein synaptophysin is fused to a pH-sensitive GFP variant, allowing visualization of exocytosis as vesicles fuse with the plasma membrane. Neurons were depolarized using a high frequency train of stimulations (20 Hz for 2 s), while the synaptic charge transfer and the exocytosis-dependent increase of fluorescence at discrete synaptic sites were monitored simultaneously (**Fig. 7a,b** and **Supplementary Fig. 8a**). Neurons were subsequently superfused with an NH_4Cl^- solution to verify the localization of synapses and to provide an estimate on their total number (**Fig. 7a,b**). Synaptic regions unmasked by NH_4Cl^- treatment were characterized according to their exocytotic activities. Synapses were considered 'active' when the fluorescence increase exceeded 3 standard deviations (s.d.) of the background noise (50 ± 0.02 (arbitrary units, au); **Fig. 7a,b**). 'Silent' synapses, instead, remained subthreshold but showed a similar fluorescence increase when superfused with NH_4Cl^- (**Fig. 7b**). Indeed, neurons cultured on ceb-ko astrocytes responded with a significantly stronger fluorescence increase than those grown on WT astrocytes (**Fig. 7c–e**). In contrast, sybII-ko astrocytes supported only a smaller depolarization-dependent fluorescence increase. Hardly any increase in fluorescence could be detected in the absence of astrocytes (**Fig. 7c–e**). In close correlation with the fluorescence analyses, we obtained corresponding changes in synaptic charge transfer (**Fig. 7f**), EPSC amplitude and RRP size (**Supplementary Fig. 8d–g**) with the accompanying electrophysiological recordings for the various groups. Quantification of the total number of synapses (determined by NH_4Cl treatment and excluding neuronal somata) revealed no changes due to either type of v-SNARE deficiency in the astrocytes, but it did reveal a strong reduction in the absence of astrocytes (**Fig. 7g**). Immunostaining with the presynaptic marker bassoon confirmed that the absence of astrocytes, but not their v-SNARE deficiency, reduced the number of synapses (**Supplementary Fig. 9**). Direct comparison of the depolarization-dependent fluorescence increase at synaptic sites (number of active synapses × ΔF/synapse) with the corresponding synaptic charge

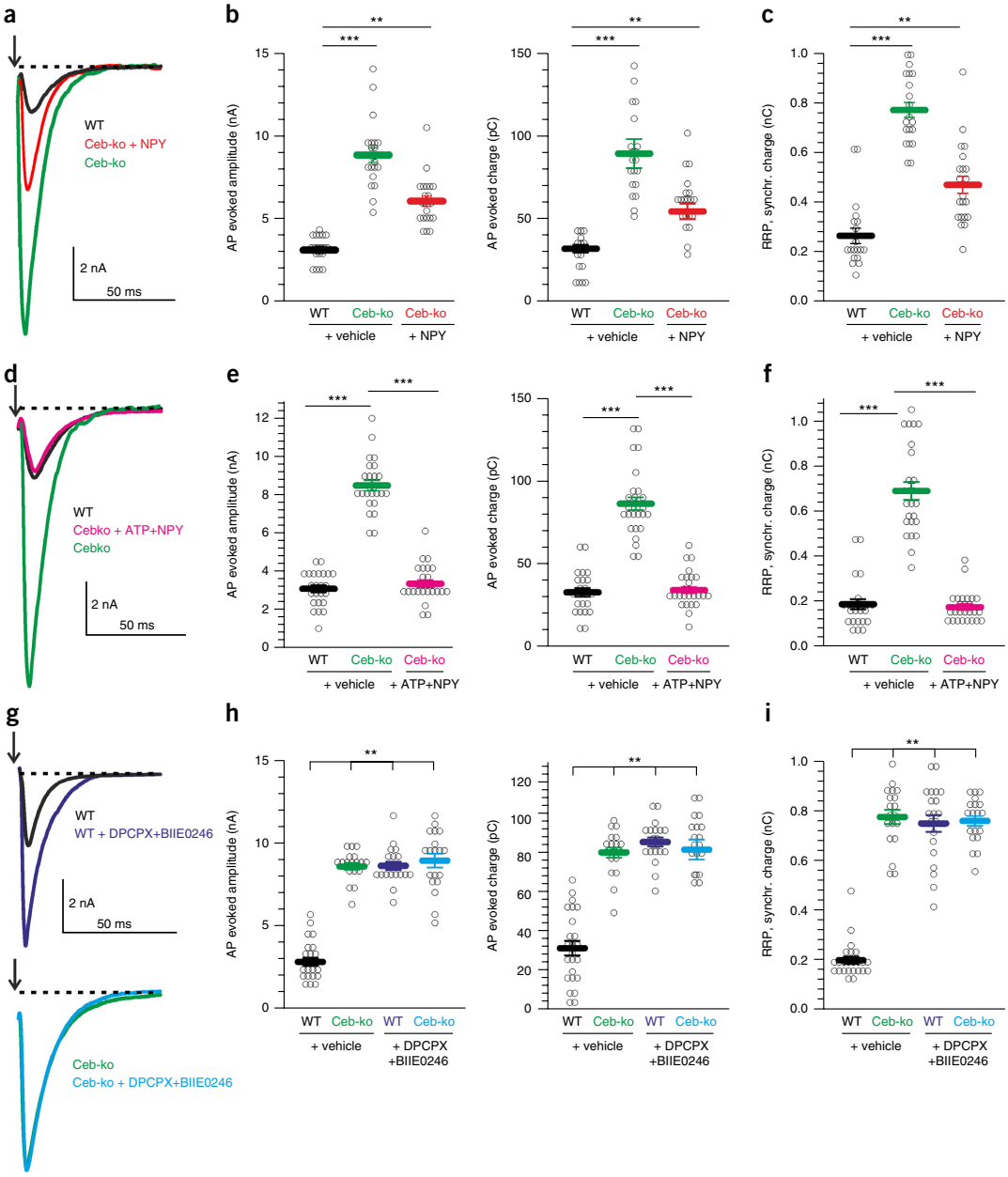

Figure 6 Extracellular application of both NPY and ATP mimics the inhibitory effect of ceb-mediated gliotransmission on neuronal signaling. (**a**) Representative traces of AP-evoked EPSC recordings in autaptic neurons plated on WT and ceb-ko astrocytes treated daily with 10 nM NPY. Arrow indicates action potential evoked depolarization. Depolarization artifacts have been omitted. (**b**,**c**) Daily application of NPY only partially restored the EPSC amplitude, charge and RRP size in neurons grown on ceb-ko astrocytes when compared to recordings from WT astrocytes (data were collected from three preparations; WT + vehicle, $n = 19$; ceb-ko + vehicle, $n = 20$; ceb-ko + NPY, $n = 21$; EPSC ampl.: WT vs. ceb-ko (vehicle), $P < 0.001$; WT vs. ceb-ko (NPY), $P = 0.01$; EPSC charge: WT vs. ceb-ko (vehicle), $P < 0.001$; ceb-ko (vehicle) vs. ceb-ko (NPY), $P = 0.01$; RRP synchronous (sync) charge: WT vs. ceb-ko (vehicle), $P = 0.0018$; WT vs. ceb-ko (NPY), $P < 0.001$; one-way ANOVA). (**d**) Exemplary traces of the AP-evoked EPSC recorded in neurons treated daily with 10 nM NPY and 10 nM ATP grown on either WT or ceb-ko astrocytes. (**e**,**f**) Evoked EPSC amplitude, charge and RRP shows that co-application of NPY and ATP fully restored the WT response (data was obtained from three preparations; WT + vehicle, $n = 24$; ceb-ko + vehicle, $n = 25$; ceb-ko + NPY+ATP, $n = 26$; AP-evoked ampl.: WT vs. ceb-ko (vehicle), $P < 0.001$; WT (vehicle) vs. ceb-ko (ATP+NPY), $P = 0.673$; ceb-ko (vehicle) vs. ceb-ko (ATP+NPY), $P < 0.001$; AP-evoked charge: WT vs. ceb-ko (vehicle), $P < 0.001$; WT (vehicle) vs. ceb-ko (ATP+NPY), $P = 0.943$; ceb-ko (vehicle) vs. ceb-ko (ATP+NPY), $P < 0.001$; RRP sync. charge: WT vs. ceb-ko (vehicle), $P < 0.001$; WT (vehicle) vs. ceb-ko (ATP+NPY), $P = 0.938$; ceb-ko (vehicle) vs. ceb-ko (ATP+NPY), $P < 0.001$, one-way ANOVA). (**g**) Sample traces of AP-evoked EPSCs for neurons cultured with WT or ceb-ko astrocytes treated daily with 150 nM adenosine-receptor antagonist DPCPX and 150 nM NPY-receptor antagonist BIIE0246. (**h**,**i**) Evoked EPSC amplitude, charge and RRP show that co-application of the antagonists increased the synaptic response recorded for WT astrocytes to that of ceb-ko cells but left the ceb-ko response unchanged (data was obtained from three preparations; WT + vehicle, $n = 24$; ceb-ko + vehicle, $n = 19$; WT+DPCPX+BIIE0246, $n = 20$; ceb-ko + DPCPX+BIIE0246, $n = 19$; AP-evoked ampl.: ceb-ko (vehicle), $P < 0.001$; WT (DPCPX+BIIE0246), $P < 0.001$; ceb-ko (DPCPX+BIIE0246), $P < 0.001$; AP-evoked charge: ceb-ko (vehicle), $P < 0.001$; WT (DPCPX+BIIE0246), $P < 0.001$; ceb-ko (DPCPX+BIIE0246), $P < 0.001$; RRP synchronous charge: ceb-ko (vehicle), $P < 0.001$; WT (DPCPX+BIIE0246), $P < 0.001$; ceb-ko (DPCPX+BIIE0246), $P < 0.001$, one-way ANOVA vs. WT). $^{**}P < 0.01$; $^{***}P < 0.001$. All data are represented as mean ± s.e.m.

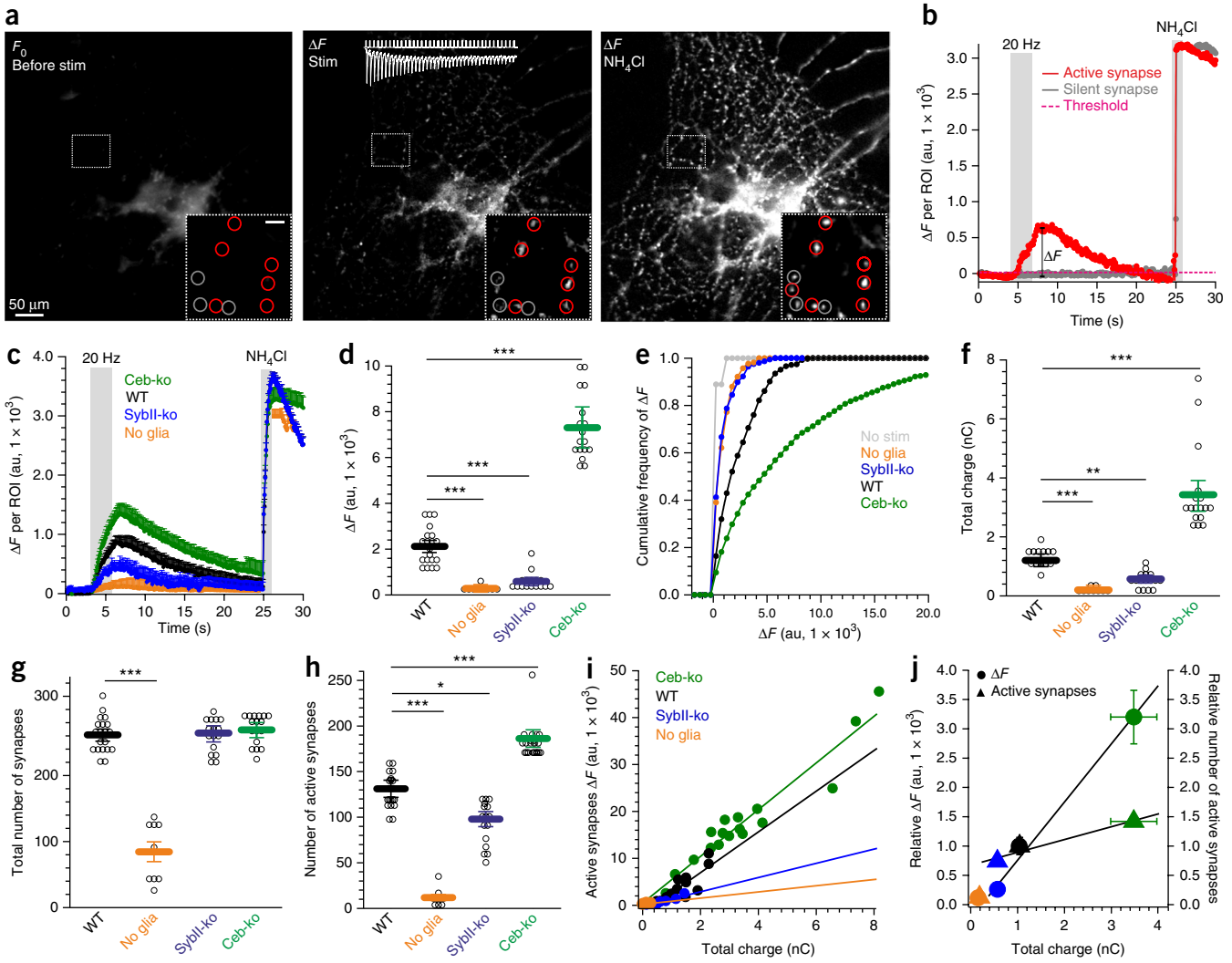

Figure 7 Astrocytes regulate synaptic strength by distinct v-SNARE-dependent secretion pathways. (**a**) Exemplary difference images (ΔF) from a WT neuron transfected with synaptophysin-pHluorin (syn-pH) before stimulation (left), during stimulation (middle) and after NH_4Cl treatment (right, scaled to 70% of ΔF). High-magnification insets illustrate exemplary active (red circle) and silent synapses (gray circle); scale bar, 5 µm. The stimulation-dependent (20 Hz for 2 s) increase of fluorescence at synaptic sites was monitored (10 Hz) simultaneously with the AP-evoked charge transfer. (**b**) Exemplary traces of an active and silent (nonresponding) synapse. Synaptic sites were determined by NH_4Cl treatment to unquench all syn-pH fluorescence. Dashed line marks 3× s.d. of background noise. (**c**) Astrocytic v-SNARE deficiency differentially regulates exocytotic activity at individual synapses (ΔF) but does not affect the subsequent NH_4Cl^--dependent unquenching response. Exocytotic activity was strongly reduced without an astrocytic feeder layer (no glia). (**d**) Mean ΔF at the end of stimulation as shown in **c** (gray bar). Note the strong increase in ΔF in neurons grown with ceb-ko astrocytes (no glia, $P < 0.001$; sybII-ko, $P < 0.001$; ceb-ko, $P < 0.001$, one-way ANOVA vs. WT). (**e**) Cumulative frequency distribution of ΔF for the indicated groups. (**f**) The total charge in neurons cultured with ceb-ko astrocytes is strongly increased, whereas it is decreased in cells grown with sybII-ko astrocytes or without glia cells (no glia, $P < 0.001$; sybII-ko, $P = 0.0032$; ceb-ko, $P < 0.001$, one-way ANOVA vs. WT). (**g**) Synaptic charge transfer for the indicated culture conditions (no glia, $P = 0.000048$; sybII-ko, $P = 0.688$; ceb-ko, $P = 0.719$, one-way ANOVA vs. WT). (**h**) Astrocytic v-SNARE deficiency affects the number of active synapses (no glia, $P < 0.001$; sybII-ko, $P = 0.001$; ceb-ko, $P < 0.001$, one-way ANOVA vs. WT). (**i**) The syn-pH response strongly correlates with the synaptic charge transfer (ceb-ko, $r^2 = 0.92$; WT, $r^2 = 0.83$; sybII-ko, $r^2 = 0.81$; no glia, $r^2 = 0.62$). (**j**) The exocytotic activity per synapse, rather than the number of active synapses, changes proportionally with the magnitude of the synaptic charge transfer (slopes: exocytotic ΔF/charge transfer, 0.96; active synapse number per charge transfer, 0.32). Data was collected from four independent preparations from WT $n = 20$; sybII-ko $n = 17$; ceb-ko $n = 16$; no glia, $n = 9$; not stimulated, $n = 5$). $^{**}P < 0.01$, $^{***}P < 0.001$. All data are represented as mean ± s.e.m.

transfer of the same neuron revealed a strict correlation between both types of secretion measurements (**Fig. 7i**), corroborating the validity of our analyses (ceb-ko, $r^2 = 0.92$; WT, $r^2 = 0.83$; sybII-ko, $r^2 = 0.81$; no glia, $r^2 = 0.62$). In comparison with controls, ceb-ko astrocytes moderately increased their number of active synapses, which were marginally diminished in sybII-ko astrocytes but strongly reduced in cultures without glia cells (**Fig. 7h**). Notably, the fluorescence increase per synapse strongly and proportionally changed with the magnitude of the synaptic charge transfer for the different v-SNARE dependencies (slope of exocytotic ΔF/charge transfer = 0.96), but the number of active synapses was found to be only slightly altered (slope of active synapse number/charge transfer = 0.32; **Fig. 7j**).

These results indicate presynaptic control of neuronal signaling by ceb- and sybII-dependent release processes from astrocytes, regulating predominantly the number of releasable vesicles per synapse. They counter the possibility of v-SNARE-dependent alterations in synapse

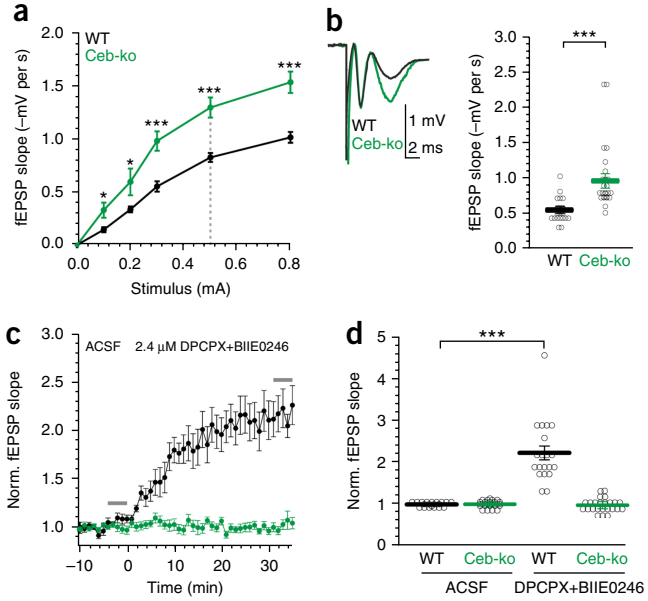

Figure 8 Ceb-mediated NPY and ATP release modulates synaptic efficacy. (**a**) The stimulation-intensity-dependent field excitatory postsynaptic potential (fEPSP) slope increase in the stratum radiatum was larger in ceb-ko mice than in WT controls (dashed line represents the stimulus strength used in **c** and **d**. (**b**) Exemplary recordings (mean of ten single traces, 0.2 Hz, stimulus 0.3 mA) illustrate the significantly increased fEPSP slope in ceb-ko mice compared with controls. (ANOVA vs. WT: 0.1 mA, $P = 0.044$; 0.2 mA, $P = 0.037$; 0.3 mA, $P = 0.002$; 0.5 mA, $P < 0.001$; 0.8 mA, $P < 0.001$). (**c**) DPCPX and BIIE0246 (2.4 µM each simultaneously) steepened the fEPSP slope in slices from WT mice but not in those from ceb-ko mice. (**d**) DPCPX+BIIE0246 significantly increased the slope of the fEPSP in WT slices. fEPSP slopes were determined at the end of the recording and normalized to responses before drug application (as indicated by the gray bars in **c**; ANOVA vs. WT, artificial cerebrospinal fluid (ACSF), $P = 0.436$; DPCPX+BIIE0246, $P < 0.001$). Data was collected from 20 slices prepared from 7 WT mice and from 29 slices prepared from 8 ceb-ko mice. * $P < 0.05$, ** $P < 0.01$, *** $P < 0.001$. All data are represented as mean ± s.e.m.

number and confirm that the general presence of astrocytes is crucial for synapse maintenance and formation, as previously shown by others[29]. In summary, the combined data demonstrate that v-SNARE-mediated release from astrocytes potently regulates the efficacy of synaptic transmission at presynaptic sites.

Astrocytes modulate synaptic transmission in acute hippocampal slices

To determine whether loss of NPY and ATP secretion also affects synaptic transmission in a more intact system, we used acutely isolated hippocampal slices from age-matched WT and *Ceb*$^{-/-}$ mice (8–11 weeks old). Notably, ceb expression in the brain is restricted mostly to non-neuronal cells, such as astrocytes or vascular cells[39]. The slope of the Schaffer-collateral-evoked field excitatory postsynaptic potentials (fEPSPs) was significantly larger in *Ceb*$^{-/-}$ mice than in WT controls (**Fig. 8a**,**b**). These results, recorded in a global *Ceb*$^{-/-}$ mouse, are in excellent agreement with our findings *in vitro*, which were caused by astrocyte-specific ceb deficiency (**Figs. 2**–**7**). Furthermore, co-application of DPCPX (2.4 µM) and BIIE0246 (2.4 µM) increased the fEPSP slope in WT but not in ceb-ko hippocampal slices (**Fig. 8c**,**d**), substantiating the results obtained with acute and chronic applications of the antagonists in glia–neuron cultures (**Fig. 6** and **Supplementary Fig. 7**). Collectively, these observations suggest that astrocytes mediate an ambient ATP and NPY level in the brain that tonically suppresses excitatory synaptic transmission.

DISCUSSION

Astrocytes contribute to virtually all aspects of brain function, including ionic homeostasis, energy metabolism and synaptic signaling. Still, substantial advances toward understanding the molecular mechanisms of gliotransmission and its impact on neuronal signaling have been often hampered by conceptual and technical limitations[11]. Taking advantage of individual null-mutants for sybII and ceb, as well as the compound null-mutant for both v-SNARE proteins, we unraveled previously undetected individual v-SNARE dependencies of astrocytic release processes and their functional impact on neuronal signaling (**Supplementary Fig. 10**). Specifically, we present strong evidence for the co-existence of independent secretion pathways in astrocytes that employ sybII and ceb as functionally non-overlapping v-SNARE proteins that antagonistically regulate fast glutamatergic neurotransmission. Thus, our work unveils molecular mechanisms by which astrocytes communicate with neurons and effectively control elementary steps of synaptic communication, providing new insights into fundamental aspects of brain function.

v-SNARE-mediated vesicular glutamate and NPY release from astrocytes

Key properties of synapses are their ability to process and spread information between neurons in an ever-changing manner. Given their close proximity and intimate contact with synapses, astrocytes are known to contribute to the regulation of the neuronal microenvironment[9]. Gliotransmission is one of several postulated ways how astrocytes can actively modulate synaptic properties[40], yet general principles regarding their release mechanisms remain unclear and controversial[10,11]. Previous studies have aimed at interfering with astrocytic SNARE proteins by using either the (dn)SNARE mouse model (which overexpresses a truncated sybII fragment[5]) or the 'iBot' mouse expressing the botulinum neurotoxin B light chain[21]. Neither these genetic mouse models nor poisoning with TeNT allowed researchers to identify the relevant v-SNARE variant or to discriminate between distinct astrocytic secretion pathways, because sybII and ceb are similarly affected by these perturbations. Taking advantage of individual null-mutants for ceb and sybII, we unraveled a bimodal regulation of synaptic signaling by astrocytes and provide direct evidence for v-SNARE-mediated release of vesicular NPY and glutamate.

Using independent experimental strategies (resorufin and iGluSnFr assay), we show that stimulation of astrocytes with DHPG evokes glutamate release, which is abolished in sybII-deficient astrocytes but unchanged in ceb-ko astrocytes. Furthermore, sybII co-localized with vGlut in the astrocytic periphery, consistent with previous reports showing that vGlut$^+$ SLMVs are found in perisynaptic processes of astrocytes[12,41]. In agreement with these results, biochemical analyses revealed that astrocytic SLMVs are positive for vGlut and vesicle-associated membrane proteins (sybII and ceb) and that they store glutamate as well as D-serine[42]. Our experiments provide the first evidence we are aware of that specifically sybII-dependent secretion in astrocytes potentiates glutamatergic neurotransmission. The differential impact of the KAR antagonist on neuronal signaling in the presence of WT (reduced EPSC amplitude) and sybII-ko astrocytes (unchanged EPSC amplitude), together with the observation that loss of astrocytic sybII specifically affects presynaptic parameters (diminished RRP, reduced P_r and increased PPF), indicate that presynaptic KARs[28] mediate the enhancement of synaptic signaling by

astrocyte-derived glutamate. This finding agrees with previous results implicating presynaptic KARs in the facilitation of synaptic signaling *in situ*[37,43], as well as in the mobilization of synaptic vesicles[44].

Since SNARE proteins may be equally important for insertion of membrane-bound ion channels like the anion channel bestrophin-1 (BEST-1)[45], dependency on SNAREs is still insufficient proof for vesicular glutamate release. However, BEST-1-mediated glutamate release was found to be insensitive to TeNT[45] and therefore cannot account for the observed sybII-dependent glutamate secretion from astrocytes. The close co-localization of sybII and vGlut and the pulsatile, quantal-like appearance of astrocytic glutamate flashes in response to mGluR activation, together with functional analyses using acute impairment of astrocytic glutamate release by TeNT poisoning[1,2,6], strongly suggest that sybII mediates glutamate release by vesicular exocytosis. Nevertheless, a potential contribution of nonvesicular processes to glutamate release from astrocytes (for example, through glutamate transporting proteins) cannot be rigorously excluded[15].

Beside stimulatory actions, astrocytic secretion has also been implicated in suppression of basal synaptic transmission[40]. We demonstrate that astrocytes constitute a second, independent secretion pathway that employs ceb and mediates Ca^{2+}-triggered vesicular NPY release from astrocytes. Loss of astrocytic ceb, which co-localizes with NPY, strongly potentiated fast glutamatergic neurotransmission, a phenotype that is specifically reverted by expression of ceb in ceb-ko astrocytes. Similarly, loss of astrocytic NPY enhanced synaptic signaling, albeit to a lesser degree, as observed with ceb-ko astrocytes. Several lines of evidence suggest that ATP serves as the second inhibitory transmitter and is released in a ceb-dependent fashion. First, ATP is stored in astrocytic LDCVs and can be found in the same subcellular fractions as the LDCV marker-proteins secretogranin II and chromogranin[33]. Second, chronic as well as acute co-application of NPY and ATP mimicked the inhibitory function of the ceb-dependent secretion pathway on neuronal signaling. Third, application of Y2- and A1-receptor antagonists reproduced the ceb-ko phenotype in WT co-cultures but had no functional consequences for neurons grown on ceb-ko astrocytes. The latter result indicates that loss of ceb-dependent NPY and ATP release accounted for the increase in synaptic transmission observed with ceb-ko cells, rather than altered glutamate transport activity in ceb-ko astrocytes[17]. Fourth, acute hippocampal slices from ceb-ko mice displayed larger synaptic responses upon Schaffer collateral stimulation and were similarly unaffected by A1- and Y2-receptor treatment.

Collectively, these results demonstrate a distinct, ceb-dependent vesicular secretion pathway in astrocytes that exerts its tonic inhibitory action on basal synaptic transmission by activation of presynaptic Y2- and A1-receptors *in vitro* and *in situ*. They further assign a previously undescribed role to ceb in a bona fide Ca^{2+}-triggered release process and demonstrate that sybII and ceb are functionally not redundant in mediating distinct secretion pathways in astrocytes.

Astrocytes: friends and foes at synapses

The autaptic culture system provides unique opportunities for comparatively analyzing the impact of different astrocytic v-SNARE deficiencies on neuronal signaling. Notably, loss of both independent secretion pathways in astrocytes scales the synaptic response to levels that closely resembled those of WT astrocytes (**Supplementary Fig. 10**). This suggests that sybII- and ceb-mediated secretion from astrocytes and their physiological consequences are well balanced, most likely maximizing the dynamic range of synaptic scaling for either excitatory and inhibitory inputs. The similar responses of WT and dko astrocytes agree with the observation that TeNT poisoning of astrocytes has no effect on basal synaptic activity[46] (but cf. ref. 47). In comparison with the single-knockout phenotypes, the similarity of these two sets of responses also emphasizes the necessity of selectively perturbing individual secretion pathways (rather than blocking secretion[46] or generally interfering with Ca^{2+} signaling[48]) to gain insight into the complex interplay between astrocytes and neurons. It is tempting to speculate that basal secretion by sybII- and ceb-mediated mechanisms generates an ambient glutamate+D-serine and NPY+adenosine tone that fine tunes synaptic scaling. This does not necessarily mean that astrocytes constitutively release gliotransmitters, but they may directly respond to spontaneous and basal neuronal signaling. Thus, astrocytes do not only provide supportive functions (for example, transmitter uptake, K^+ clearance, pH homeostasis, trophic support) but also homeostatically regulate synaptic efficacy. Astrocytic secretion may represent a powerful mechanism for shifting the set point of synaptic circuits. Alterations in the balanced excitation and inhibition by astrocytic signaling may adjust the set point and thereby contribute to synaptic plasticity and heterosynaptic modulation[40].

In contrast to v-SNARE deficiencies, the absence of astrocytes strongly reduced the total number of synapses. Evidently, v-SNARE-dependent gliotransmission provides a level of synaptic regulation that substantially differs from the generally supporting actions of astrocytes in regulating synaptogenesis and synapse maintenance[38].

Our results provide strong evidence for presynaptic regulation of fast neuronal signaling by astrocytes. First, high-frequency stimulation protocols and application of hypertonic sucrose solution demonstrated that loss of ceb-mediated astrocytic release strongly increased the RRP size. In contrast, loss of sybII-dependent glutamate release substantially diminished the RRP, reduced the P_r and increased the PPF. Second, experiments with synaptophysin-pHluorin provided direct evidence that astrocytes regulate the presynaptic secretion process. Third, neither v-SNARE deficiency affected the properties of quantal signaling, indicative of unchanged postsynaptic signal generation. Furthermore, our results are consistent with previous reports implicating astrocytic glutamate release in potentiating neurotransmission through activation of presynaptic glutamate receptors[2,6,22]. Moreover, astrocytic ATP release (after conversion to adenosine), as well as acute NPY application, has been implicated in neuronal suppression by modulation of presynaptic Ca^{2+} entry[49] and the protein kinase A pathway[50].

Overall, our results elucidate cellular mechanisms for the functional heterogeneity of astrocyte signaling in the central nervous system. These processes may be relevant for behavior control (e.g., sleep regulation) and may also participate in the antiepileptogenic and neuroprotective action of NPY on intense neural activity. Given that perisynaptic astrocytic processes can contact more than 10,000 synaptic sites[8] within the territory of a single astrocyte, local as well as paracrine actions of gliotransmission are likely to occur.

In summary, our observations unveil opposing actions of astrocytes that are well-suited to fine-tune fast glutamatergic neurotransmission. They offer a new conceptual framework for studying astrocyte–neuron interactions and glial heterogeneity in the brain.

METHODS

Methods, including statements of data availability and any associated accession codes and references, are available in the online version of the paper.

Note: Any Supplementary Information and Source Data files are available in the online version of the paper.

ACKNOWLEDGMENTS

The authors thank J. Rettig, D. Stevens, M. Dhara and R. Mohrmann for valuable discussions. We thank W. Frisch, V. Schmidt and M. Wirth for excellent technical assistance. The work was supported by grants from the DFG (SFB 894, TRR 152 and SPP 1757) to D.B. and F.K. and from HOMFOR (to Y.S.).

AUTHOR CONTRIBUTIONS

Y.S. performed *in vitro* and *in situ* experiments; N.Z. and F.K. performed slice recordings and commented on the manuscript. Y.S. and D.B. designed the research and wrote the manuscript.

COMPETING FINANCIAL INTERESTS

The authors declare no competing financial interests.

1. Henneberger, C., Papouin, T., Oliet, S.H. & Rusakov, D.A. Long-term potentiation depends on release of D-serine from astrocytes. *Nature* **463**, 232–236 (2010).
2. Jourdain, P. *et al.* Glutamate exocytosis from astrocytes controls synaptic strength. *Nat. Neurosci.* **10**, 331–339 (2007).
3. Panatier, A. *et al.* Glia-derived D-serine controls NMDA receptor activity and synaptic memory. *Cell* **125**, 775–784 (2006).
4. Parpura, V. *et al.* Glutamate-mediated astrocyte-neuron signalling. *Nature* **369**, 744–747 (1994).
5. Pascual, O. *et al.* Astrocytic purinergic signaling coordinates synaptic networks. *Science* **310**, 113–116 (2005).
6. Perea, G. & Araque, A. Astrocytes potentiate transmitter release at single hippocampal synapses. *Science* **317**, 1083–1086 (2007).
7. Zhang, J.M. *et al.* ATP released by astrocytes mediates glutamatergic activity-dependent heterosynaptic suppression. *Neuron* **40**, 971–982 (2003).
8. Halassa, M.M., Fellin, T., Takano, H., Dong, J.H. & Haydon, P.G. Synaptic islands defined by the territory of a single astrocyte. *J. Neurosci.* **27**, 6473–6477 (2007).
9. Araque, A. *et al.* Gliotransmitters travel in time and space. *Neuron* **81**, 728–739 (2014).
10. Sahlender, D.A., Savtchouk, I. & Volterra, A. What do we know about gliotransmitter release from astrocytes? *Phil. Trans. R. Soc. Lond. B* **369**, 20130592 (2014).
11. Verkhratsky, A., Matteoli, M., Parpura, V., Mothet, J.P. & Zorec, R. Astrocytes as secretory cells of the central nervous system: idiosyncrasies of vesicular secretion. *EMBO J.* **35**, 239–257 (2016).
12. Bezzi, P. *et al.* Astrocytes contain a vesicular compartment that is competent for regulated exocytosis of glutamate. *Nat. Neurosci.* **7**, 613–620 (2004).
13. Ramamoorthy, P. & Whim, M.D. Trafficking and fusion of neuropeptide Y-containing dense-core granules in astrocytes. *J. Neurosci.* **28**, 13815–13827 (2008).
14. Stellwagen, D. & Malenka, R.C. Synaptic scaling mediated by glial TNF-alpha. *Nature* **440**, 1054–1059 (2006).
15. Hamilton, N.B. & Attwell, D. Do astrocytes really exocytose neurotransmitters? *Nat. Rev. Neurosci.* **11**, 227–238 (2010).
16. Crippa, D. *et al.* Synaptobrevin2-expressing vesicles in rat astrocytes: insights into molecular characterization, dynamics and exocytosis. *J. Physiol. (Lond.)* **570**, 567–582 (2006).
17. Li, D. *et al.* Astrocyte VAMP3 vesicles undergo Ca^{2+} -independent cycling and modulate glutamate transporter trafficking. *J. Physiol. (Lond.)* **593**, 2807–2832 (2015).
18. Martineau, M. Gliotransmission: focus on exocytotic release of L-glutamate and D-serine from astrocytes. *Biochem. Soc. Trans.* **41**, 1557–1561 (2013).
19. Schubert, V., Bouvier, D. & Volterra, A. SNARE protein expression in synaptic terminals and astrocytes in the adult hippocampus: a comparative analysis. *Glia* **59**, 1472–1488 (2011).
20. Wolfes, A.C. *et al.* A novel method for culturing stellate astrocytes reveals spatially distinct Ca2+ signaling and vesicle recycling in astrocytic processes. *J. Gen. Physiol.* **149**, 149–170 (2017).
21. Slezak, M. *et al.* Relevance of exocytotic glutamate release from retinal glia. *Neuron* **74**, 504–516 (2012).
22. Fellin, T. *et al.* Neuronal synchrony mediated by astrocytic glutamate through activation of extrasynaptic NMDA receptors. *Neuron* **43**, 729–743 (2004).
23. Marvin, J.S. *et al.* An optimized fluorescent probe for visualizing glutamate neurotransmission. *Nat. Methods* **10**, 162–170 (2013).
24. Guzman, R.E., Schwarz, Y.N., Rettig, J. & Bruns, D. SNARE force synchronizes synaptic vesicle fusion and controls the kinetics of quantal synaptic transmission. *J. Neurosci.* **30**, 10272–10281 (2010).
25. Bacci, A., Huguenard, J.R. & Prince, D.A. Differential modulation of synaptic transmission by neuropeptide Y in rat neocortical neurons. *Proc. Natl. Acad. Sci. USA* **99**, 17125–17130 (2002).
26. Gómez-Gonzalo, M. *et al.* Endocannabinoids induce lateral long-term potentiation of transmitter release by stimulation of gliotransmission. *Cereb. Cortex* **25**, 3699–3712 (2015).
27. Navarrete, M. & Araque, A. Endocannabinoids potentiate synaptic transmission through stimulation of astrocytes. *Neuron* **68**, 113–126 (2010).
28. Sihra, T.S. & Rodríguez-Moreno, A. Presynaptic kainate receptor-mediated bidirectional modulatory actions: mechanisms. *Neurochem. Int.* **62**, 982–987 (2013).
29. Ullian, E.M., Sapperstein, S.K., Christopherson, K.S. & Barres, B.A. Control of synapse number by glia. *Science* **291**, 657–661 (2001).
30. Otsu, Y. *et al.* Competition between phasic and asynchronous release for recovered synaptic vesicles at developing hippocampal autaptic synapses. *J. Neurosci.* **24**, 420–433 (2004).
31. Rosenmund, C. & Stevens, C.F. Definition of the readily releasable pool of vesicles at hippocampal synapses. *Neuron* **16**, 1197–1207 (1996).
32. Baraban, S.C., Hollopeter, G., Erickson, J.C., Schwartzkroin, P.A. & Palmiter, R.D. Knock-out mice reveal a critical antiepileptic role for neuropeptide Y. *J. Neurosci.* **17**, 8927–8936 (1997).
33. Coco, S. *et al.* Storage and release of ATP from astrocytes in culture. *J. Biol. Chem.* **278**, 1354–1362 (2003).
34. Dunwiddie, T.V. & Masino, S.A. The role and regulation of adenosine in the central nervous system. *Annu. Rev. Neurosci.* **24**, 31–55 (2001).
35. Parker, S.L. & Balasubramaniam, A. Neuropeptide Y Y2 receptor in health and disease. *Br. J. Pharmacol.* **153**, 420–431 (2008).
36. Pinheiro, P.S. & Mulle, C. Presynaptic glutamate receptors: physiological functions and mechanisms of action. *Nat. Rev. Neurosci.* **9**, 423–436 (2008).
37. Chittajallu, R., Braithwaite, S.P., Clarke, V.R. & Henley, J.M. Kainate receptors: subunits, synaptic localization and function. *Trends Pharmacol. Sci.* **20**, 26–35 (1999).
38. Pfrieger, F.W. Role of glial cells in the formation and maintenance of synapses. *Brain Res. Rev.* **63**, 39–46 (2010).
39. Zhang, Y. *et al.* An RNA-sequencing transcriptome and splicing database of glia, neurons, and vascular cells of the cerebral cortex. *J. Neurosci.* **34**, 11929–11947 (2014).
40. De Pittà, M., Brunel, N. & Volterra, A. Astrocytes: orchestrating synaptic plasticity? *Neuroscience* **323**, 43–61 (2016).
41. Bergersen, L.H. *et al.* Immunogold detection of L-glutamate and D-serine in small synaptic-like microvesicles in adult hippocampal astrocytes. *Cereb. Cortex* **22**, 1690–1697 (2012).
42. Martineau, M. *et al.* Storage and uptake of D-serine into astrocytic synaptic-like vesicles specify gliotransmission. *J. Neurosci.* **33**, 3413–3423 (2013).
43. Contractor, A. *et al.* Loss of kainate receptor-mediated heterosynaptic facilitation of mossy-fiber synapses in KA2-/- mice. *J. Neurosci.* **23**, 422–429 (2003).
44. Gelsomino, G. *et al.* Kainate induces mobilization of synaptic vesicles at the growth cone through the activation of protein kinase A. *Cereb. Cortex* **23**, 531–541 (2013).
45. Woo, D.H. *et al.* TREK-1 and Best1 channels mediate fast and slow glutamate release in astrocytes upon GPCR activation. *Cell* **151**, 25–40 (2012).
46. Lee, H.S. *et al.* Astrocytes contribute to gamma oscillations and recognition memory. *Proc. Natl. Acad. Sci. USA* **111**, E3343–E3352 (2014).
47. Panatier, A. *et al.* Astrocytes are endogenous regulators of basal transmission at central synapses. *Cell* **146**, 785–798 (2011).
48. Agulhon, C., Fiacco, T.A. & McCarthy, K.D. Hippocampal short- and long-term plasticity are not modulated by astrocyte Ca^{2+} signaling. *Science* **327**, 1250–1254 (2010).
49. Moore, K.A., Nicoll, R.A. & Schmitz, D. Adenosine gates synaptic plasticity at hippocampal mossy fiber synapses. *Proc. Natl. Acad. Sci. USA* **100**, 14397–14402 (2003).
50. Wang, S. *et al.* Adenosinergic depression of glutamatergic transmission in the entorhinal cortex of juvenile rats via reduction of glutamate release probability and the number of releasable vesicles. *PLoS One* **8**, e62185 (2013).

ONLINE METHODS

Ethics statement. All experimental procedures were approved and performed in accordance with EU guidelines and the ethic regulations of the animal welfare committee at the University of Saarland. All efforts were made to minimize animal suffering and to reduce the number of animals used.

Hippocampal astrocyte and neuronal cultures. Hippocampal astrocytes were prepared from E18.5 *SynaptobrevinII*$^{-/-}$, *Cellubrevin*$^{-/-}$, *Synaptobrevin II/Cellubrevin*$^{-/-}$, *NPY*$^{-/-}$[32] and age-matched wild-type mice of either sex as described previously[13]. Mice were housed at a 12-h light/12-h dark cycle (3–4 animals per cage). Autaptic cultures of hippocampal neurons were prepared from WT, *SybII*$^{-/-}$ or *NPY*$^{-/-}$ mice at E18.5–P1 as described previously[24]. Only islands with single neurons were used for electrophysiological recordings after 7–10 DIC.

Viral constructs/lentiviral transfection. cDNAs encoding for sybII, ceb, NPY, syn-pH and iGluSnFr (Addgene #41732) were subcloned into the pRRL.sin.CPPT.CMV.WPRE lentiviral transfer vector[24]. All constructs were verified by DNA sequence analysis (MWG Germany). Lentiviral particles were produced as previously described[24]. Primary astrocytes or neurons were transfected with 50–100 µL of viral suspension 1–2 DIC. For rescue experiments in autaptic cultures, astrocytes were transfected before plating of neurons.

Immunostaining. Astrocytes, plated on collagen-coated (1 mg/mL) coverslips, were fixed for 10 min at room temperature (20–22 °C) in PBS containing 2% paraformaldehyde. Cells were quenched for 10 min with 50 mM NH_4Cl in PBS and blocked for 30 min in PBS containing 3% BSA and 0.1% Triton-X 100. Primary antibodies (anti-sybII, 1:1,000, mouse monoclonal 69.1, kindly provided by R. Jahn, MPI for Biophysical Chemistry, Göttingen; anti-cellubrevin, 1:1,000, polyclonal, rabbit TG21, kindly provided by T. Galli (University of Paris, France); anti-NPY, 1:500, mouse monoclonal Santa Cruz, USA, Cat. No. sc-133080; anti-bassoon, 1:500, Synaptic Systems, Cat. No. 141 011; and anti-vGlut, 1:500, rabbit polyclonal, anti-vGlut1/2, Synaptic Systems, Cat. No. 135 503) and secondary antibodies (1:1,000, Alexa Fluor 555- and 488-conjugated goat anti-mouse or goat anti-rabbit; Invitrogen) were diluted in blocking buffer. Cells were incubated with primary and secondary antibodies overnight and for 1.5 h at RT, respectively. After mounting in glycerol, cells were imaged by confocal microscopy (LSM 710; Carl Zeiss) using AxioVision 2008 software (Carl Zeiss) and a 100× 1.3-NA oil objective. For LSM images, pixel size and pixel dwell time was 0.110 µm and 3.15 µs. The following filter sets were used: Zeiss 09 (BP 450-490, FT 510, LP 515), Zeiss 15 (BP 546/12, FT 580, LP 590) and Zeiss 38 (BP 470/40, FT 495, LP BP 525/50). Images were analyzed with the software package ImageJ (version 1.45) and SigmaPlot 8.0 (Systat Software, Inc.). To determine the number of synapses, the images were subjected to a uniform background (25 ± 1.2 au) subtraction. Presynaptic bassoon$^+$ puncta were manually counted (using a grid of 3 × 3-pixel regions of interest) on the entire autaptic neuron. The antibody specificity was validated in **Supplementary Figure 2** (anti-sybII, anti-ceb and anti-NPY) and for anti-vGlut and anti-bassoon by the supplier.

NPY secretion experiments. Astrocytes from the indicated genotypes were plated onto collagen-coated (1 mg/mL) coverslips and transfected with NPYmTFP. For rescue experiments, either sybII-mRFP or ceb-mRFP was co-transfected with NPYmTFP. Cells were imaged 7–9 DIC by confocal microscopy (LSM 710; Carl Zeiss) using AxioVision 2008 software (Carl Zeiss) and a 100× 1.3-NA oil objective at room temperature. To elicit NPY release, astrocytes were stimulated by superfusion with Ringer's solution containing 1 mM glutamate using a custom-made perfusion pipette. Signals were recorded at 2.5 Hz using a time-series protocol in AxioVision2008. Images were background-subtracted and analyzed with the software package ImageJ (version 1.45) and SigmaPlot 12 (Systat Software, Inc.). NPY puncta were determined within a predefined region of interest (50 × 50 µm) and tracked over consecutive images to follow the exocytotic loss of NPY in response to stimulation.

Glutamate secretion experiments. Glutamate secretion was measured according to the previously described procedure[21] using a modified Amplex Red Glutamic Acid Kit (Invitrogen) protocol. Cells were incubated in extracellular solution containing (in mM): 140 NaCl, 2.4 KCl, 2 $CaCl_2$, 2 $MgCl_2$, 10 HEPES, 10 D-glucose, pH 7.3 with NaOH, osmolarity 310 mOsm, with 100 mM Amplex Red reagent, 0.5 U/mL horse radish peroxidase, 0.16 U/mL L-glutamate oxidase, 1.0 U/mL L-glutamate pyruvate transaminase and 400 mM L-alanine. Cells were stimulated using 10 µM DHPG and imaged with a Zeiss LSM 710 using AxioVision 2008 software (Carl Zeiss) and a 40× oil objective at RT. To capture fluorescent resorufin molecules, cells were coated with 0.1% agarose immediately after stimulation. Resorufin fluorescence (488-nm excitation, 515-nm emission) was recorded at 1 Hz using a time-series protocol. Subsequent images were analyzed with the software package ImageJ (version 1.48) and SigmaPlot 12 (Systat Software, Inc.). Peak amplitudes were calculated as the difference between mean fluorescence intensities before and after the stimulus within the cell.

For the iGluSnFr experiments, transfected astrocytes were visualized with a Zeiss Plan Apochromat 40× oil immersion objective (NA 1.3) at 488 nm excitation (PolychromeV, TILL Photonics) using an EMCCD camera (Visitron, Germany). Cells were stimulated with 20 µM DHPG and were subjected to 1 mM glutamate at the end of the experiment to determine the expression level of the sensor. Images were analyzed with the software package ImageJ (version 1.48). Images were background-subtracted and normalized to the initial fluorescence (F_0 = average of three prestimulus images). Regions of interest (2 × 2 µm) were identified and fluorescence changes ($\Delta F/F_0$) were tracked throughout the entire stack. Fluorescence signals were further analyzed with a custom-written routine in IgorPro 6. Only events exceeding 5× s.d. of the noise (WT s.d.: $0.0156 \pm 1.3 \times 10^{-3}$; ceb-ko s.d.: $0.0181 \pm 3.2 \times 10^{-3}$) were analyzed.

Ca^{2+} measurements in astrocytes. Astrocytes (7–10 DIC) were incubated in extracellular solution containing 10 µM Fluo4am (Invitrogen) for 20 min at 37 °C. Afterwards, cells were washed with extracellular solution and imaged using a Zeiss LSM 710 and AxioVision 2008 software (Carl Zeiss) and a 40× oil objective at room temperature. Fluorescence changes were recorded at 1 Hz using a time-series protocol. Cells were stimulated with 1 mM glutamate at the indicated time point. Images were analyzed with the software package ImageJ (version 1.48) and SigmaPlot 12 (Systat Software, Inc.). Fluorescence amplitudes were calculated as difference between mean fluorescence intensities before and after the stimulus in a cell; the nucleus was omitted from the quantification.

Drug treatment. All chemicals were purchased from Sigma-Aldrich unless stated otherwise. For chronic agonist and antagonist treatment ATP (10 nM), NPY (10 nM), DPCPX (150 nM) and BIIE0246 (150 nM) were bath applied to the autaptic neurons at 1 DIC and subsequently added daily. For acute treatment, ATP/NPY (10 µM), DPCPX/BIIE0246 (500 nM) and NS-102 (3 µM, Tocris, Germany) neurons were rapidly superfused using a gravity-fed fast-flow system.

Electrophysiological measurements of synaptic currents. Whole-cell voltage-clamp recordings of synaptic currents were obtained from isolated autaptic neurons. All experiments were performed on age-matched neurons derived from mice of the same litter. Patch pipettes (R_{tip} 4–5.5 MΩ) were filled with intracellular solution containing (in mM): 137.5 potassium-gluconate, 11 NaCl, 2 MgATP, 0.2 Na_2GTP, 1.1 EGTA, 11 HEPES, 11 D-glucose, pH 7.3 with KOH. We used the standard extracellular solution, containing (in mM) 130 NaCl, 10 $NaHCO_3$, 2.4 KCl, 2 $CaCl_2$, 2 $MgCl_2$, 10 HEPES, 10 D-glucose, pH 7.3 with NaOH, osmolarity 299 mOsm. D-2-amino-5-phosphonopentanoate (APV; 50 µM) was added to inhibit NMDA receptors and prevent synaptic plasticity changes. To minimize the potential contribution of GABAergic currents, the reversal potential of chloride-mediated currents was adjusted to the holding potential. To verify the recording of AMPA-receptor (AMPAR) currents, exemplary neurons were superfused with 25 µM DNQX (data not shown). Neurons were voltage clamped at −70 mV with an EPC10 amplifier (HEKA Electronic) under the control of Pulse 8.5 software (HEKA Electronic) and stimulated by membrane depolarizations to +10 mV for 0.7 ms every 5 s (0.2 Hz). We analyzed cells with an average access resistance of 6–15 MΩ, with 75–80% resistance compensation and >100 pA leak-current. Current signals were low-pass filtered at 2.9 kHz (four-pole Bessel filter EPSC10) and digitized at a rate of 10 or 50 kHz. Spontaneous mEPSCs were recorded before stimulation. AP-evoked EPSC amplitudes and charges were determined from the average of 10 EPSCs recorded at 0.2 Hz.

The readily releasable pool (RRP) was determined by a 5-s application of hypertonic sucrose solution (500 mM) using a gravity-fed fast-flow system. To calculate the RRP size, the current integral was corrected by subtracting the steady-state

doi:10.1038/nn.4647

current component (determined at the end of the of hypertonic sucrose application) that probably reflects steady-state vesicle replenishment and exocytosis during hypertonic challenges[31]. The charge of an AP-evoked response within a train was quantified by integrating the current for 46.5 ms following each pulse after subtracting a baseline value measured 1–2 ms before the stimulus. Synchronous release was determined by subtracting the integral of the steady-state current component (i.e., the asynchronous charge) determined at the end of the response. To determine mEPSC properties with reasonable fidelity and to prevent the detection of 'false events' (due to random noise fluctuations), spontaneous mEPSCs with a peak amplitude >15 pA and a charge criterion >25 fC were analyzed using commercial software (Mini Analysis, Synaptosoft, Version 6.0.3).

Slice preparation. Coronal hippocampal slices 350 µm thick were prepared from WT and ceb-ko mice (8–11 weeks) of either sex. Mice were deeply anesthetized with isoflurane (AbbVie, Germany) and decapitated at the second cervical vertebra. The brain was rapidly removed from the skull and chilled with ice-cold sucrose-based artificial cerebrospinal fluid (ACSF) containing (in mM): 87 NaCl, 3 KCl, 1.25 NaH_2PO_4, 0.5 $CaCl_2$, 3 $MgCl_2$, 25 $NaHCO_3$, 25 glucose and 75 sucrose, saturated with 95% O_2/5%CO_2. The brain was cut with a vibratome (Leica, Germany), the hippocampus was microdissected and slices were incubated in ACSF containing (in mM): 126 NaCl, 3 KCl, 25 $NaHCO_3$, 15 glucose, 1.2 NaH_2PO_4, 2 $CaCl_2$ and 2 $MgCl_2$ for 30 min at 30 °C. Subsequently, slices were kept at room temperature (RT) with continuous oxygenation before use.

Slice electrophysiology. Slices were transferred into a recording chamber, mounted on an upright microscope (Zeiss, Germany) and continuously superfused (2 mL/min) with ACSF containing 1 mM $MgCl_2$ and 2.5 mM $CaCl_2$, saturated with 95% O_2/5% CO_2. Field potentials from the CA1 stratum radiatum were recorded with an extracellular low resistance glass pipette (2–2.5 M) filled with ACSF. To block inhibitory transmission, recordings were made in the presence of 50 µM picrotoxin. To stimulate the Schaffer collaterals, a concentric bipolar tungsten electrode (MicroProbes, USA) was placed in the stratum radiatum near the CA1 border. fEPSP slopes of evoked synaptic potentials were measured from averaged (n = 8–12) sweeps recorded at 0.1 Hz. Recordings were performed with an EPSC 10 amplifier (HEKA, Germany). Signals were filtered at 2 kHz and digitized at 5 kHz. Recordings were analyzed offline using custom-written macros in IgorPro 6.3 (WaveMetrics). Genotypes of the animals were confirmed by PCR from tail biopsies after each experiment. For drug application, the fEPSP slopes were normalized to the average slope before drug application.

Imaging synaptophysin-pHluorin responses. Syn-pH fluorescence was acquired with an Evolve EMCCD camera (Visitron, Germany) using a Zeiss Plan Apochromat 40× oil immersion objective (NA 1.3). Autaptic neurons were stimulated with 20 Hz for 2 s. At the end of the experiment, the neuron was subjected to alkaline imaging buffer (50 mM NH_4Cl substituted for 50 mM NaCl) to reveal total syn-pH fluorescence. Fluorescent images were captured at 10 Hz with custom-written macros in VisiView (Visitron, Germany), processed offline using ImageJ 1.43 and SigmaPlot 12. The background subtraction was done by subtracting the F_0 image (average of three prestimulus images) from all subsequent images ($\Delta F_n = F_n - F_0$). Regions of interest of identical size were placed over single synapses visible upon NH_4Cl treatment to track the fluorescence intensity over time. Regions that responded to the AP stimulation with a fluorescence increase 3× s.d. of noise (3 × 50 au) were considered active synapses. Somatic regions were omitted from the analysis.

Statistical analysis. Values are given as means ± s.e.m. To determine statistically significant differences, one-way ANOVA and Student's t test were used for comparing groups, unless otherwise indicated. The similarities of variances between groups were tested when performing statistics in SigmaPlot, and statistical tests were chosen accordingly. Normality was tested (Shapiro-Wilk). Multiple comparisons were performed using the Tukey-Kramer *post hoc* test. No statistical methods were used to predetermine sample sizes; however, sample sizes are similar to those reported in previous publications[24]. Data collection and analyses were not performed blind to the experimental condition, and no method of randomization was applied.

Data availability. The data that support the findings of the study are available from the corresponding author upon reasonable request.

A **Life Science Reporting Summary** is available.

nature research

Corresponding author(s): Dieter Bruns

☐ Initial submission ☐ Revised version ☒ Final submission

Life Sciences Reporting Summary

Nature Research wishes to improve the reproducibility of the work that we publish. This form is intended for publication with all accepted life science papers and provides structure for consistency and transparency in reporting. Every life science submission will use this form; some list items might not apply to an individual manuscript, but all fields must be completed for clarity.

For further information on the points included in this form, see Reporting Life Sciences Research. For further information on Nature Research policies, including our data availability policy, see Authors & Referees and the Editorial Policy Checklist.

Experimental design

1. Sample size

Describe how sample size was determined.

No statistical methods were used to predetermine sample sizes; however, sample sizes were similar to those reported in previous publications (Guzman et al., 2010; Borisovska et al., 2012; Dhara et al., 2016).

2. Data exclusions

Describe any data exclusions.

No data exclusion was done.

3. Replication

Describe whether the experimental findings were reliably reproduced.

Experiments were repeated in at least three independent preparations. Individual numbers of replication are described in the Reporting Checklist.

4. Randomization

Describe how samples/organisms/participants were allocated into experimental groups.

No method of randomization was done.

5. Blinding

Describe whether the investigators were blinded to group allocation during data collection and/or analysis.

Data collection and analyses were not performed blind to the experimental condition.

Note: all studies involving animals and/or human research participants must disclose whether blinding and randomization were used.

6. Statistical parameters

For all figures and tables that use statistical methods, confirm that the following items are present in relevant figure legends (or in the Methods section if additional space is needed).

n/a	Confirmed
☐	☒ The exact sample size (*n*) for each experimental group/condition, given as a discrete number and unit of measurement (animals, litters, cultures, etc.)
☐	☒ A description of how samples were collected, noting whether measurements were taken from distinct samples or whether the same sample was measured repeatedly
☐	☒ A statement indicating how many times each experiment was replicated
☐	☒ The statistical test(s) used and whether they are one- or two-sided (note: only common tests should be described solely by name; more complex techniques should be described in the Methods section)
☐	☒ A description of any assumptions or corrections, such as an adjustment for multiple comparisons
☐	☒ The test results (e.g. *P* values) given as exact values whenever possible and with confidence intervals noted
☐	☒ A clear description of statistics including central tendency (e.g. median, mean) and variation (e.g. standard deviation, interquartile range)
☐	☒ Clearly defined error bars

See the web collection on statistics for biologists for further resources and guidance.

Nature Neuroscience: doi:10.1038/nn.4647

Software

Policy information about availability of computer code

7. Software

Describe the software used to analyze the data in this study.	IgorPro 6.37; ImageJ 1.48; SigmaPlot 13

For manuscripts utilizing custom algorithms or software that are central to the paper but not yet described in the published literature, software must be made available to editors and reviewers upon request. We strongly encourage code deposition in a community repository (e.g. GitHub). *Nature Methods* guidance for providing algorithms and software for publication provides further information on this topic.

Materials and reagents

Policy information about availability of materials

8. Materials availability

Indicate whether there are restrictions on availability of unique materials or if these materials are only available for distribution by a for-profit company.	No unique materials were used in this study. All materials are comercially available.

9. Antibodies

Describe the antibodies used and how they were validated for use in the system under study (i.e. assay and species).	Anti-SybII, 1:1000, mouse monoclonal 69.1 (specificity verified in Supp.Fig. 2; provided by R.Jahn, MPI Göttingen; Synaptic Systems #104211) Anti-cellubrevin, 1:1000, polyclonal, rabbit TG21 (specificity verified in Supp.Fig. 2; kindly provided by T. Galli, Paris) Anti-NPY, 1:500, mouse monoclonal Santa Cruz, USA, Cat. No. sc-133080 (specificity verified in Supp.Fig.2) Anti-bassoon, 1:500, Synaptic Systems, Cat. No. 141 011 (Specificity verified by supplier) Anti-vGlut, 1:500, Synaptic Systems, Cat. No. 135 503 (Specificity verified by supplier)

10. Eukaryotic cell lines

a. State the source of each eukaryotic cell line used.	Not applicable
b. Describe the method of cell line authentication used.	Not applicable
c. Report whether the cell lines were tested for mycoplasma contamination.	Not applicable
d. If any of the cell lines used are listed in the database of commonly misidentified cell lines maintained by ICLAC, provide a scientific rationale for their use.	Not applicable

Animals and human research participants

Policy information about studies involving animals; when reporting animal research, follow the ARRIVE guidelines

11. Description of research animals

Provide details on animals and/or animal-derived materials used in the study.	Synaptobrevin II-ko (Schoch et al., 2001), Synabrevin/cellubrevin-dko (Borisovska et al., 2005), Cellubrevin-ko (Yang et al., 2001) and NPY-ko mice (Baraban et al., 1997) were continously back-crossed with C57BL/6N. Mice of either sex were used for cell culture preparations and slice recordings.

Policy information about studies involving human research participants

12. Description of human research participants

Describe the covariate-relevant population characteristics of the human research participants.	Not applicable

Nature Neuroscience: doi:10.1038/nn.4647